polymers

MDPI

Communication

Tuning Microparticle Porosity during Single Needle Electrospraying Synthesis via a Non-Solvent-Based Physicochemical Approach

Yuan Gao [1,2], Yuntong Bai [1,2], Ding Zhao [1,2], Ming-Wei Chang [1,2,*], Zeeshan Ahmad [3] and Jing-Song Li [1,2]

Received: 25 September 2015; Accepted: 27 November 2015; Published: 21 December 2015
Academic Editor: Michael D. Guiver

1 College of Biomedical Engineering & Instrument Science, Zhejiang University, Hangzhou 310027, China; 21315080@zju.edu.cn (Y.G.); baiutouxt@gmail.com (Y.B.); dr_zhao@zju.edu.cn (D.Z.); ljs@zju.edu.cn (J.-S.L.)
2 Zhejiang Provincial Key Laboratory of Cardio-Cerebral Vascular Detection Technology and Medicinal Effectiveness Appraisal, Zhejiang University, Hangzhou 310027, China
3 Leicester School of Pharmacy, De Montfort University, The Gateway, Leicester LE1 9BH, UK; zahmad@dmu.ac.uk
* Correspondence: mwchang@zju.edu.cn; Tel./Fax: +86-571-8795-1517

Abstract: Porous materials, especially microparticles (MP), are utilized in almost every field of engineering and science, ranging from healthcare materials (drug delivery to tissue engineering) to environmental engineering (biosensing to catalysis). Here, we utilize the single needle electrospraying technique (as opposed to complex systems currently in development) to prepare a variety of poly(ε-caprolactone) (PCL) MPs with diverse surface morphologies (variation in pore size from 220 nm to 1.35 μm) and architectural features (e.g., ellipsoidal, surface lamellar, Janus lotus seedpods and spherical). This is achieved by using an unconventional approach (exploiting physicochemical properties of a series of non-solvents as the collection media) via a single step. Sub-micron pores presented on MPs were visualized by electron microscopy (demonstrating a mean MP size range of 7–20 μm). The present approach enables modulation in morphology and size requirements for specific applications (e.g., pulmonary delivery, biological scaffolds, multi-stage drug delivery and biomaterial topography enhancement). Differences in static water contact angles were observed between smooth and porous MP-coated surfaces. This reflects the hydrophilic/hydrophobic properties of these materials.

Keywords: microparticles; porous; shape; poly(ε-caprolactone); tuned

1. Introduction

Porous microparticles (MPs) have well-established applications across all biomedical and physical science disciplines; ranging from drug delivery and biomaterials [1] to environmental sensing and catalysis [2,3]. The porous nature of MPs provides an increased surface area-to-volume ratio, lower density and improved permeability compared to solid MPs of equivalent size. More recently, porous particles with desirable biocompatibilities (e.g., prepared from suitable synthetic polymers: poly(ε-caprolactone) (PCL), poly(D,L-lactic-*co*-glycolic acid) (PLGA) or poly(L-lactide) (PLA)) [4] have shown appreciable potential as biological scaffolds for tissue regeneration and orthopaedic applications [5,6].

Conventionally, the preparation of porous MPs has been achieved using template-assisted processing, porogen leaching methods, emulsion polymerization, self-assembly diffusion, reactive

sintering methods and controlled solvent evaporation routes [7–9]. The electrospraying (ES) technique is a less common method for preparing porous MP structures, with the established modulation mechanism based on the solvent (polymer vehicle) evaporation rate. This technique has several advantages over existing processes: it avoids complex synthesis procedures where the loss of material is significant; a relatively narrow particle size distribution is achievable; and ambient conditions during synthesis. The process can also be scaled up to increase the output rate as required [10,11]. Previous experiments by Wu *et al.* evidenced the validity of the ES technique for porous MP synthesis. Here, PCL-chloroform droplets (prepared by using ES) were collected in water, which yielded nano-sized micropore and micro-sized macropore concurrence on the MP surface [12]. More recently, porous polymethylmethacrylate (PMMA)-based microstructures were obtained using several non-solvents and solvent (dichloromethane (DCM)) mixtures (suspensions) via co-ES. In this instance, both solid and hollow MPs with a porous surface topology were formed [13]. While the use of multiple non-solvents (for material dissolution) and multiple nozzles (e.g., co-axial methods) is valuable, the complexity of these systems will contribute towards greater costs and additional parameter analysis (both for output and pre-process characterization) [14,15]. In this study, we demonstrate an unconventional approach using a series of collecting non-solvents, although the base solvent (DCM) for PCL solubilisation remains constant. When using this approach, non-solvents' varying physicochemical properties (e.g., surface tension, viscosity and vapour pressure) are exploited to create MPs with tailored porosity and hydrophobicity, which is devoid of multiple precursor solutions, synthesis steps and processing needles. For this study, FDA-approved biocompatible and biodegradable PCL polymer was used [16].

2. Experimental Section

2.1. Materials

Poly(ε-caprolactone) (PCL, 45 kDa) was obtained from Sigma-Aldrich (St. Louis, MO, USA). Dichloromethane (DCM) was supplied by Sinopharm Chemical Reagent Co., Ltd., Shanghai, China. A series of organic solvents, including methanol, ethanol, 1,2-propanediol, *n*-butanol and tetraethyl orthosilicate (TEOS), were used as collection media, obtained from Sinopharm Chemical, China. Deionized water (DI water) was produced with a Millipore Milli-Q Reference ultra-pure water purifier (Milford, MA, USA). All chemicals were of the analytic grade and used without further treatment.

2.2. Methods

2.2.1. PCL Solution Preparation

PCL was dissolved in DCM at a concentration of 3 wt % by mechanical stirring (VELP ARE heating magnetic stirrer, Usmate Velate, Italy) for 1 h to allow homogenous dissolution and subsequently used for the ES process.

2.2.2. Preparation of Microparticles

MPs were fabricated via the ES technique using the apparatus depicted in Figure 1. The liquid was propelled by an infuser pump (KD Scientific KDS100, Holliston, MA, USA) at a feeding rate of 4.2 $mL \cdot h^{-1}$ into a metallic stainless steel needle (inner diameter: 0.8 mm; outer diameter: 1 mm). ES was enabled by applying a controlled electrical field (Glassman high voltage Inc. series FC, High Bridge, NJ, USA) to the processing head (16 kV). Under the action of an optimized electrical force, fine droplets resulting from the ejected fluid jet (under cone-jet mode) were collected at a distance of 13 cm in various collection media (non-solvents). One millimetre of collection medium was pipetted onto a glass slide substrate, and sprayed droplets were collected directly on to the deposited medium for 10 s. The MPs resulting from solidification were transferred to a desiccator and kept for 1 week to

ensure complete dryness for further characterization. MPs were collected directly from the desiccator for microscopy.

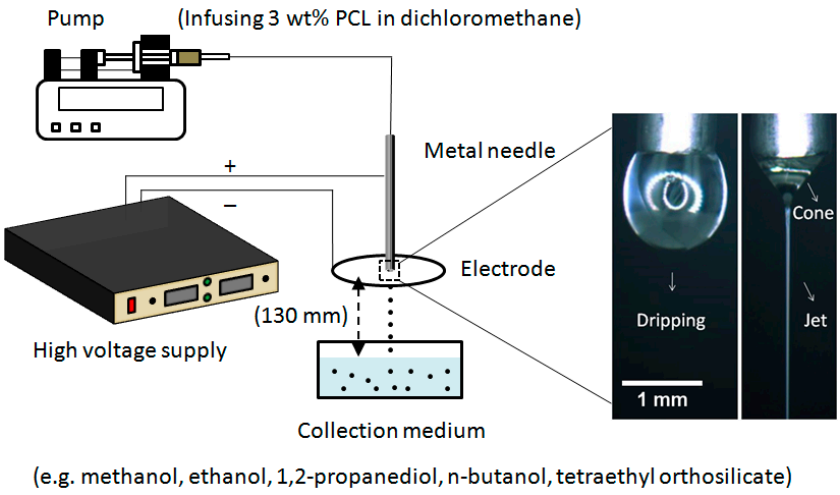

Figure 1. Schematic illustration of typical electrospraying (ES) setup. The inset shows two characteristic jetting modes during ES: dripping mode and cone-jet mode.

2.2.3. Microparticle Characterization

MP morphology was characterized using scanning electron microscopy (SEM ProX, Phenom, Eindhoven, Netherlands). Samples were sputter coated with a layer of gold (90 s) and scanned at an acceleration voltage of 15 kV. The MP size was obtained using SEM imaging by averaging 100 randomly-selected measurements for each MP specimen (sample variation based on different collecting non-solvents) using the image analysis software ImageJ (National Institute of Health, Austin, TX, USA). Similarly, the statistic distributions of pores presented on the porous particles were analysed based on 300 measurements for each sample.

2.2.4. Surface Measurements and Solvent Characterizations

Static water contact angle measurements were performed at room temperature using an optical contact angle and interface tension meter (SL200KB, Kino Industry CO. Ltd., Norcross, GA, USA). A deionized water droplet (1 μL) was carefully dripped onto the MP-deposited glass substrates, and contact angle values were calculated by averaging the results of three separate positions for each experimental condition. The viscosity of various organic solutions (25 °C) was determined with a DV2TRV viscometer (Brookfield, Middleboro, MA, USA), and the surface tension was measured at 20 °C by an automatic tensiometer (HengPing instrument, Shanghai, China). For the evaluation, solvent molecular weight and vapour pressure were obtained from chemical library data [17].

3. Results and Discussion

The preparation of porous MP via the ES technique is driven by the phase separation process, which occurs between distinct material phases. Mass and thermal exchange are the main driving forces during solvent evaporation and its diffusion through polymer [18]. While the process is affected by material type and their properties (*i.e.*, solute, solvent, additives), in relation to ES, it is also influenced by experimental parameters (e.g., solute concentration, collection distance) and the surrounding environments (e.g., temperature, humidity) [19,20]. For this reason, all experiments were performed under identical conditions (as listed above) with the exception of the collecting media.

MPs with diverse morphologies and topologies were obtained. A series of organic non-solvents, methanol, ethanol, 1,2-propanediol, *n*-butanol and tetraethyl orthosilicate (TEOS), were selected as

variable collection media. For the ease of description, MPs prepared using these were denoted as P_{met}, P_{eth}, P_{pro}, P_{but} and P_{teos}, respectively. SEM images (Figure 2) highlight morphological variations. Figure 2a shows MPs collected in methanol, where most MPs possess an ellipsoidal shape with many discrete macropores distributed on their surface, in addition to some dimpled features. Such structures have great potential in tissue engineering, as they possess appreciable porosity, as well as polymeric strut networks throughout the MP structure, which allow them to have mechanical features. The pores in these systems allow for removal and uptake of vital nutrients, and as the MP matrix is biodegradable, integration into tissue is possible [21]. In contrast, P_{eth} MPs show a more continuous and denser porous structure (Figure 2b). In this instance, pores are well established, and most MPs here display a hemispherical shape, with smaller MPs demonstrating spherical morphologies. As the pores are more pronounced, compromising PCL strut components, P_{eth} MPs are ideal candidates for pulmonary drug delivery, as the reduced particle density (therefore, ideal aerodynamic diameter) will allow better manoeuvring of these particles within the airways of several drug administration components (e.g., oral cavity, windpipe and bronchi) [22]. Previous studies have shown the utility of highly porous MPs (e.g., using PLGA) as delivery systems compared to existing aerosolized dosage forms [23].

A more distinct morphological variation arises when MPs are formed in 1,2-propanediol. P_{pro} MPs with a flower-like surface texture were observed (Figure 2c). The presence of many lamellate protrusions greatly increases the MP surface roughness, which is ideal for attachment to biological (cellular) structures [24]. Previous studies have demonstrated the role of topography (roughness and chemistry) in cell-material interactions [25], and as ES has been utilized to prepare biomaterial coatings (e.g., using PCL), enhancing the surface-cell interaction will be achievable using P_{pro} MPs. Unique lotus seedpod-shaped particles were obtained for P_{but} (Figure 2d), with numerous shallow spherical pores distributed discretely on the surface plane component of each MP, while the spherical surface component is non-porous and smooth. In effect, these "Janus" structures are ideal for advanced drug delivery [26]. Porous structures increase the permeability of drug from the polymeric matrix; hence, a two-tier release profile is expected as the smooth non-porous surface will release drugs at a slower rate [27].

Exquisite spherical particles were derived under the deployment of TEOS (Figure 2e). P_{teos} MPs display uniform spherical pores on their surface, and when compared to P_{met}- and P_{eth}-based MPs, their structures are more uniform and more well defined. In this regard, these MPs are candidates for both pulmonary drug delivery and tissue scaffold applications [28].

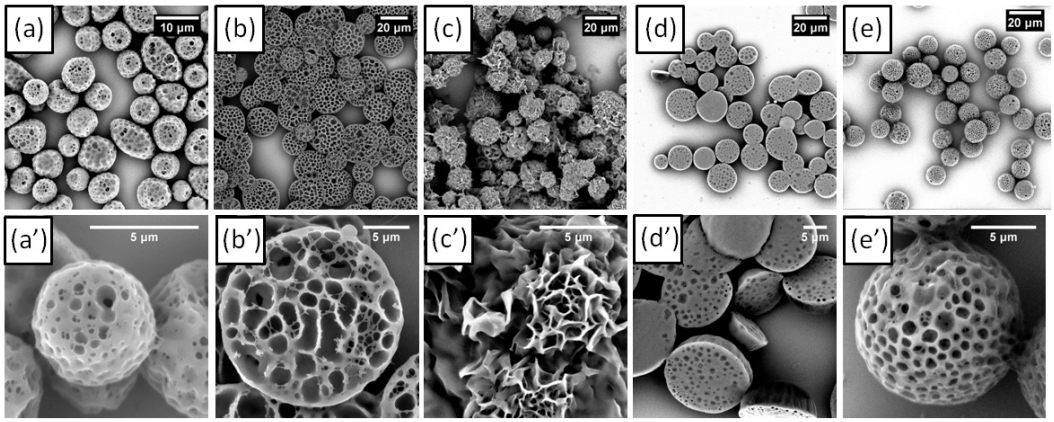

Figure 2. SEM images of poly(ε-caprolactone) (PCL)-dichloromethane (DCM) microparticles (MPs) collected in the organic solvent (non-solvents): (**a**) methanol; (**b**) ethanol; (**c**) 1,2-propanediol; (**d**) *n*-butanol; (**e**) tetraethyl orthosilicate. (**a′**–**e′**) High-magnification images showing the surface detail of the same porous MPs from (**a**–**e**), respectively.

Statistical analysis of the various MP systems was based on 100 random measurements, and the mean particle diameter (Figure 3a) was 7.0 ± 1.18, 20.35 ± 4.48, 12.55 ± 2.19, 12.83 ± 2.53 and 11.7 ± 1.42 μm for P_{met}, P_{eth}, P_{pro}, P_{but} and P_{teos}, respectively. It can be observed that the mean particle diameter increased with non-spherical deformation and became relatively larger with the increasing pore volume, but still is within the range of 7–20 μm. The pore size distribution also varied for each MP type (Figure 3b). P_{met} exhibited the smallest mean pore size (diameter 0.22 ± 0.18 μm) and was mostly concentrated below 300 nm. The pore distribution on P_{eth} MPs presented a bimodal and comparatively scattered distribution due to the presence of low level pores (0.40 ± 0.17 μm) on the inner wall (PCL struts) of surface macro-pores (1.35 ± 0.61 μm). P_{but} and P_{teos} showed relatively uniform pore size distributions of 0.56 ± 0.33 and 0.49 ± 0.13 μm, respectively.

In addition to pore size (structural) -driven applications, surface morphological differences may also have other implications. As the PCL composition (3 wt %) was identical for all MPs (including base solvent, DCM), the divergent surface microstructure of each MP can be confirmed through changes in water contact angle measurements (CA) [29]. It should be noted that electrosprayed MPs were maintained in a desiccator to completely remove the remaining residual solvent (after jet-break up and secondary whipping motions) and collection media; thus, the influence of CA is mainly dominated by the MP surface microstructure. It is reported that the presence of surface pores increases CA due to improved surface roughness, which facilitates air entrapment within voids at the polymer-liquid interface, especially for the hierarchical type, which correlates with our findings. Figure 3c exhibits the static water contact angle (CA) at various MP-deposited surfaces. P_{met}, P_{but} and P_{teos} have a CA of 81.00° ± 2.76°, 88.10° ± 5.46° and 76.26° ± 1.86°, respectively, while P_{eth}, with a bimodal pore size distribution, displayed super-hydrophobic properties with the greatest CA value of 128.39° ± 5.23°. However, the CA for P_{pro} was the lowest for all prepared MPs (43.70° ± 6.27°). This can be explained by the P_{pro} MPs collecting into irregular clusters, spontaneously, as observed during experimentation. This results in comparatively easier water penetration between MP voids and, thus, spreading.

All collection media are non-solvents for PCL, but possess good miscibility with DCM, and as a result, electrosprayed MPs were interfaced by the collection liquid. This provided time for diffusion before solidification [30]. This also explains the enhanced porosities present in all five MP samples.

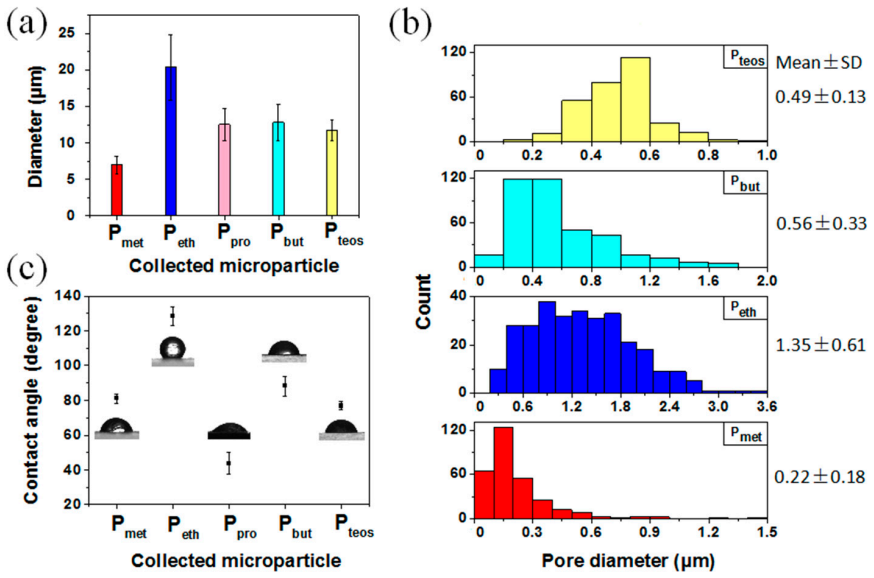

Figure 3. Statistical summary of the various MPs prepared. (**a**) Mean MP size distribution; (**b**) pore diameter distribution; and (**c**) water contact angle of layered MPs with different surface morphologies. P_{met}, P_{eth}, P_{pro}, P_{but} and P_{teos} represent particles collected in methanol, ethanol, 1,2-propanediol, *n*-butanol and tetraethyl orthosilicate (TEOS), respectively.

Figure 4 summarizes the microstructures obtained during the modified ES process. In conventional ES, ejected droplets (wet) undergo a solidification process, which involves shrinkage due to rapid drying of the base solvent [20]. In this study, DCM (vapour pressure: 47.40 kPa at 20 °C) vaporization from MPs (from needle exit to collecting substrate) led to an increased polymer concentration near the surface with a reduced surface temperature, resulting in solidification [31]. The droplet to MP transition process could potentially undergo thermally-induced phase separation (TIPS) in the absence of ambient condition regulation. Furthermore, in this study, 3 wt % PCL was utilized, which permits shell integrity, where a lower PCL concentration could have caused porous MP structures to collapse. By integrating non-solvent collection liquid contact with MPs prior to complete evaporation (of DCM), the phase separation between residual DCM and PCL polymeric chains was enhanced due to non-solvent-induced phase separation (NIPS). This enabled porous microstructure control and generation. The interplay between semi-solidified MPs and non-solvent collection media is responsible for the formation of porous microstructures, thus the physical properties of each solution are critical for the proposed mechanism(s). Several crucial non-solvent physical parameters were determined (Table 1).

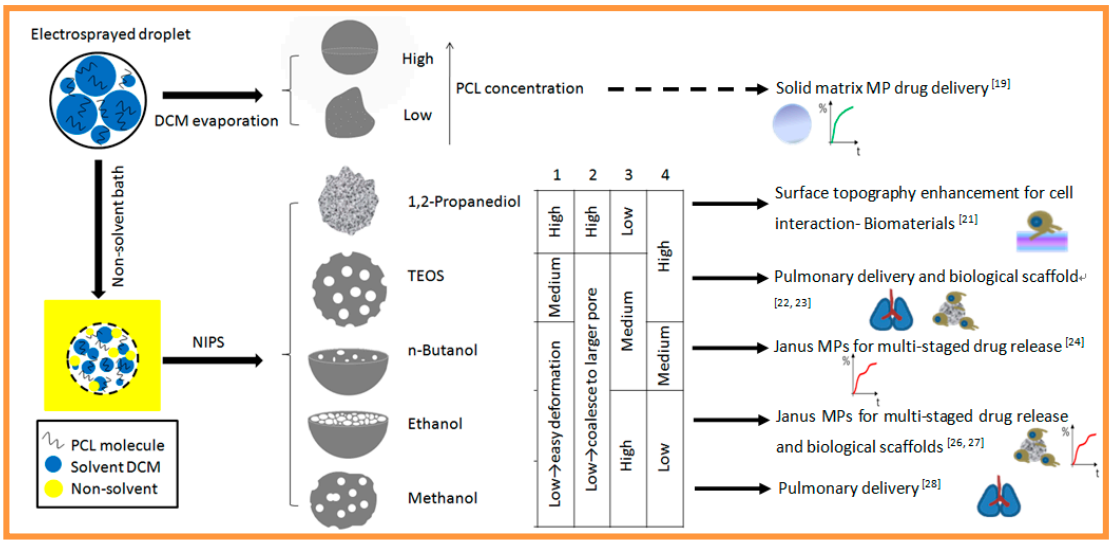

Figure 4. Schematic summary of the formation mechanism and application of diverse MPs derived with the aid of various non-solvent collecting media. Nos. 1–4 stands for solution viscosity, surface tension, vapour pressure and molecular weight of the non-solvent, respectively. NIPS, non-solvent-induced phase separation.

Table 1. Physical properties of solvents used during porous microparticle production. TEOS, tetraethyl orthosilicate.

Items	Molecular Weight ($g \cdot mol^{-1}$)	Vapour Pres [a] (kPa)	Surface Tension [b] ($mN \cdot m^{-1}$)	Viscosity [c] ($mPa \cdot s$)
Methanol	32	12.97	22.6	0.6
Ethanol	46	5.87	22.3	1.2
1,2-Propanediol	76	~0	72.0	60.5
n-Butanol	74	0.58	24.6	2.1
TEOS	208	0.13	23.4	17.9
DCM	85	47.40	23.1	0.4

[a] Saturated vapour pressure: 20 °C; [b] surface tension: 20 °C; [c] viscosity: 25 °C.

Specifically, P_{met}, P_{eth} and P_{but} MPs experienced relatively severe deformation and exhibited non-spherical structures. This may be attributed to comparatively low viscosities of methanol,

ethanol and *n*-butanol (0.6, 1.2 and 2.1 mPa·s at 25 °C, respectively). TEOS medium possesses a viscosity of 17.9 mPa·s (at 25 °C), and the corresponding MPs remained spherical in shape, but with relatively discontinuous macro-pores on their surface. 1,2-Propanediol has the highest viscosity and surface tension amongst all selected non-solvents, and consequently, P_{pro} MPs displayed no pores, but instead, flower-like textured surfaces with increased roughness, dramatically different from the other four MPs.

From the pore magnitude and depth perspective, the surface tension, viscosity and molecular size of non-solvents are crucial. According to previous experiments conducted by Gao *et al.*, non-solvents with higher surface tensions tend to diffuse into the centre of a droplet; non-solvents with lower viscosities tend to coalesce mutually and are conducive to nuclei growth. However, taking into account the molecular weight of non-solvents, relatively larger molecules will hinder the mass transfer rate and, thus, hinder nuclei growth [13]. Therefore, although methanol, ethanol, *n*-butanol and TEOS possess similar surface tensions, MPs prepared using P_{met} and P_{eth} (with lower molecular weights) exhibit deeper and connected pores compared to P_{but} and P_{teos} (larger molecular weight).

The substrate medium is an independent variable in this study. Prior to collection, there is rapid evaporation of the base solvent (from polymer-vehicle droplets), giving rise to the formation of PCL MPs via the supersaturation effect (e.g., as the DCM evaporates, the PCL polymer precipitates). MPs generated without non-solvent collecting substrates are smooth when collecting on plain glass substrates and are partially solidified with some residual solvent (DCM) remaining. The mechanism of pore formation is heavily dependent on the phase separation once the interaction occurs with the various non-solvent systems. From the micrographs obtained, porous MPs can be classed as solid foam-type structures. Residual solvent interaction with non-solvent substrates gives rise to a multi-compartment system (e.g., polymer, solvent vehicle and non-solvent substrate). Furthermore, the non-solvent (e.g., collecting media substrate) has the potential to generate voids, as nano-droplets become embedded onto the structures and are in greater quantities compared to the residual solvent [12].

Particle formation based on solvent evaporation (when using established technologies, such as spray drying) and solute movement (e.g., diffusion) has been studied extensively. The ratio between these properties led to the conceptual development of a "Péclet" number, which is dimensionless and is utilized to explain low density particles, such as porous MPs. This takes into account various material properties, such as the solvent evaporation rate and the diffusion coefficient (solute); and the value obtained is indicative of particle porosity (e.g., >1 demonstrates porous characteristics).

In this regard, electrosprayed MPs (PCL-DCM) without any collection substrate would demonstrate a low Péclet number, as MPs were smooth with no porosity and also demonstrated virtually no crumpling or buckling (low surface enrichment). However, as this study focused on non-solvent substrates, the application of a Péclet number becomes complex, as there are two solvents; residual solvent from the partially-dried MPs and the non-solvent substrate. Furthermore, due to the immiscibility between PCL and the anti-solvents deployed, the system is more likely to function as a multi-phase system, and the mechanism of pore formation will be driven by small non-solvent droplet interaction with immiscible PCL polymer particles, which subsequently dry. The inclusion of the non-solvent substrate as a deposition medium also provides the potential for convective flow; therefore, tailoring and predicting particle outcomes cannot be performed as one dimensional, and many assumptions applied to such systems (e.g., no interactions) cannot therefore be neglected [32].

Although several mechanisms exist based on the direction of flux to and from the surface of the initial and drying droplet, the combinatorial effects of non-solvent substrate-derived MP systems can be described in terms of heat and mass transfer, where the process is driven by differences in the vapour pressure of the solvents and their partial pressures. Hence, the processes based on these compartments can be attributed to two main mechanisms; thermally-induced phase separation and evaporation-induced phase separation. During the solvent evaporation phase, the polymeric droplets

become unstable, which leads to a disparity in polymeric phases. This gives rise to rich and poor regions, which is further expedited by the presence of non-solvent droplets, which localize into the drying matrix, leaving pores. The rich polymeric regions are struts, and the poor regions develop into pores.

Few studies have reported on the ES process in relation to collecting media variations. The interaction between collection medium and macromolecular mass, energy and momentum during ES is yet to be fully characterized. Further explorations will now focus on exploiting this new approach to fabricate homogeneous, multi-functional and porous particles for drug delivery on a large-scale through facile synthesis. Relevant applications of such structures will be further investigated in other biomedical material streams, such as tissue engineering and cell-topography studies.

4. Conclusions

While there have been various engineering and material (polymeric and inorganic) developments in the ES remit, fundamental process parameters have been utilized largely for experimentation. For both polymeric and inorganic materials, porous material utility, especially in the biomedical field, is becoming increasingly important. This study demonstrates that ES is a convenient and efficient method for the controlled preparation of porous polymeric microparticles. By varying the collecting medium (non-solvent) only and using the same quantity and type of polymer (*i.e.*, PCL), a broad range of MPs can be prepared to suit a series of biomedical applications. The difference in structures is driven by phase separation, using non-solvents with discrepant physical properties (*i.e.*, viscosity, surface tension and molecular weight). In addition to meeting the structural needs, MPs also display varying hydrophobicities due to air entrapment in the pore surface, which has an impact at the interface with water.

Acknowledgments: This work was financially supported by the National Nature Science Foundation of China (81301304), The Central Universities (2013QNA5003) and the Research Fund for The Doctoral Program of Higher Education of China (20130101120170).

Author Contributions: Yuan Gao and Yuntong Bai performed the experimental work. Ding Zhao, Zeeshan Ahmad and Jing-Song Li analysed and interpreted much of the data. Ming-wei Chang directed and supervised the research. All authors revised the manuscript and approved the final version.

Conflicts of Interest: The authors declare no conflict of interest.

References

1. Oh, Y.J.; Lee, J.; Seo, J.Y.; Rhim, T.; Kim, S.H.; Yoon, H.J.; Lee, K.Y. Preparation of budesonide-loaded porous PLGA microparticles and their therapeutic efficacy in a murine asthma model. *J. Control. Release* **2011**, *150*, 56–62. [CrossRef] [PubMed]
2. Thomas, A.; Kuhn, P.; Weber, J.; Titirici, M.M.; Antonietti, M. Porous polymers: Enabling solutions for energy applications. *Macromol. Rapid Commun.* **2009**, *30*, 221–236. [CrossRef] [PubMed]
3. Wang, J.; Zhao, J.; Li, Y.B.; Yang, M.; Chang, Y.Q.; Zhang, J.P.; Sun, Z.W.; Wang, Y.P. Enhanced light absorption in porous particles for ultra-NIR-sensitive biomaterials. *ACS Macro Lett.* **2015**, *4*, 392–397. [CrossRef]
4. Kim, H.K.; Park, T.G. Comparative study on sustained release of human growth hormone from semi-crystalline poly(L-lactic acid) and amorphous poly(D,L-lactic-*co*-glycolic acid) microspheres: Morphological effect on protein release. *J. Control. Release* **2004**, *98*, 115–125. [CrossRef] [PubMed]
5. Hong, S.J.; Yu, H.S.; Kim, H.W. Tissue engineering polymeric microcarriers with macroporous morphology and bone-bioactive surface. *Macromol. Biosci.* **2009**, *9*, 639–645. [CrossRef] [PubMed]
6. Pan, J.M.; Wu, R.R.; Dai, X.H.; Yin, Y.J.; Pan, G.Q.; Meng, M.J.; Shi, W.D.; Yan, Y.S. A hierarchical porous bowl-like PLA@MSNs-COOH composite for pH-dominated long-term controlled release of doxorubicin and integrated nanoparticle for potential second treatment. *Biomacromolecules* **2015**, *16*, 1131–1145. [CrossRef] [PubMed]
7. Reignier, J.; Huneault, M.A. Preparation of interconnected poly(epsilon-caprolactone) porous scaffolds by a combination of polymer and salt particulate leaching. *Polymer* **2006**, *47*, 4703–4717. [CrossRef]

8. Lee, Y.S.; Lim, K.S.; Oh, J.E.; Yoon, A.R.; Joo, W.S.; Kim, H.S.; Yun, C.O.; Kim, S. Development of porous PLGA/PEI1.8k biodegradable microspheres for the delivery of mesenchymal stem cells (MSCs). *J. Control. Release* **2015**, *205*, 128–133. [CrossRef] [PubMed]
9. Takai, C.; Hotta, T.; Shiozaki, S.; Boonsongrit, Y.; Abe, H. Unique porous microspheres with dense core and a porous layer prepared by a novel S/O/W emulsion technique. *Chem. Commun.* **2009**, 5533–5535. [CrossRef] [PubMed]
10. Chang, M.W.; Stride, E.; Edirisinghe, M. A new method for the preparation of monoporous hollow microspheres. *Langmuir* **2010**, *26*, 5115–5121. [CrossRef] [PubMed]
11. Fantini, D.; Zanetti, M.; Costa, L. Polystyrene microspheres and nanospheres produced by electrospray. *Macromol. Rapid Commun.* **2006**, *27*, 2038–2042. [CrossRef]
12. Wu, Y.Q.; Clark, R.L. Controllable porous polymer particles generated by electrospraying. *J. Colloid Interface Sci.* **2007**, *310*, 529–535. [CrossRef] [PubMed]
13. Gao, J.F.; Li, W.; Wong, J.S.P.; Hu, M.J.; Li, R.K.Y. Controllable morphology and wettability of polymer microspheres prepared by nonsolvent assisted electrospraying. *Polymer* **2014**, *55*, 2913–2920. [CrossRef]
14. Labbaf, S.; Deb, S.; Cama, G.; Stride, E.; Edirisinghe, M. Preparation of multicompartment sub-micron particles using a triple-needle electrohydrodynamic device. *J. Colloid Interface Sci.* **2013**, *409*, 245–254. [CrossRef] [PubMed]
15. Roh, K.H.; Martin, D.C.; Lahann, J. Biphasic Janus particles with nanoscale anisotropy. *Nat. Mater.* **2005**, *4*, 759–763. [CrossRef] [PubMed]
16. De la Ossa, D.H.P.; Ligresti, A.; Gil-Alegre, M.E.; Aberturas, M.R.; Molpeceres, J.; Di Marzo, V.; Suarez, A.I.T. Poly-epsilon-caprolactone microspheres as a drug delivery system for cannabinoid administration: Development, characterization and *in vitro* evaluation of their antitumoral efficacy. *J. Control. Release* **2012**, *161*, 927–932. [CrossRef] [PubMed]
17. Liu, G.Q.; Ma, L.X.; Liu, J. *Chemistry and Chemical Engineering Physical Property Data Handbook*; Chemical Industry Press: Beijing, China, 2002.
18. Feng, J.T.; Lin, L.; Chen, P.P.; Hua, W.D.; Sun, Q.M.; Ao, Z.; Liu, D.S.; Jiang, L.; Wang, S.T.; Han, D. Topographical binding to mucosa-exposed cancer cells: Pollen-mimetic porous microspheres with tunable pore sizes. *ACS Appl. Mater. Interfaces* **2015**, *7*, 8961–8967. [CrossRef] [PubMed]
19. Bohr, A.; Yang, M.S.; Baldursdottir, S.; Kristensen, J.; Dyas, M.; Stride, E.; Edirisinghe, M. Particle formation and characteristics of celecoxib-loaded poly(lactic-*co*-glycolic acid) microparticles prepared in different solvents using electrospraying. *Polymer* **2012**, *53*, 3220–3229. [CrossRef]
20. Xie, J.W.; Lim, L.K.; Phua, Y.Y.; Hua, J.S.; Wang, C.H. Electrohydrodynamic atomization for biodegradable polymeric particle production. *J. Colloid Interface Sci.* **2006**, *302*, 103–112. [CrossRef] [PubMed]
21. Wang, Y.J.; Shi, X.T.; Ren, L.; Wang, C.M.; Wang, D.A. Porous poly(lactic-*co*-glycolide) microsphere sintered scaffolds for tissue repair applications. *Mater. Sci. Eng.* **2009**, *29*, 2502–2507. [CrossRef]
22. Courrier, H.M.; Butz, N.; Vandamme, T.F. Pulmonary drug delivery systems: Recent developments and prospects. *Crit. Rev. Ther. Drug Carr. Syst.* **2002**, *19*, 425–498. [CrossRef]
23. Yang, Y.; Bajaj, N.; Xu, P.; Ohn, K.; Tsifansky, M.D.; Yeo, Y. Development of highly porous large PLGA microparticles for pulmonary drug delivery. *Biomaterials* **2009**, *30*, 1947–1953. [CrossRef] [PubMed]
24. Huang, S.; Wang, Y.J.; Deng, T.Z.; Jin, F.; Liu, S.X.; Zhang, Y.J.; Feng, F.; Jin, Y. Facile modification of gelatin-based microcarriers with multiporous surface and proliferative growth factors delivery to enhance cell growth. *J. Alloy. Compd.* **2008**, *460*, 639–645. [CrossRef]
25. Lee, J.H.; Lee, C.S.; Cho, K.Y. Enhanced cell adhesion to the dimpled surfaces of golf-ball-shaped microparticles. *ACS Appl. Mater. Interfaces* **2014**, *6*, 16493–16497. [CrossRef] [PubMed]
26. Jing, Y.; Liu, J.M.; Ji, W.H.; Wang, W.; He, S.H.; Jiang, X.Z.; Wiedmann, T.; Wang, C.; Wang, J.P. Biocompatible Fe–Si nanoparticles with adjustable self-regulation of temperature for medical applications. *ACS Appl. Mater. Interfaces* **2015**, *7*, 12649–12654. [CrossRef] [PubMed]
27. Kim, H.K.; Chung, H.J.; Park, T.G. Biodegradable polymeric microspheres with "open/closed" pores for sustained release of human growth hormone. *J. Control. Release* **2006**, *112*, 167–174. [CrossRef] [PubMed]
28. Lee, J.; Oh, Y.J.; Lee, S.K.; Lee, K.Y. Facile control of porous structures of polymer microspheres using an osmotic agent for pulmonary delivery. *J. Control. Release* **2010**, *146*, 61–67. [CrossRef] [PubMed]
29. Liu, B.; He, Y.N.; Fan, Y.; Wang, X.G. Fabricating super-hydrophobic lotus-leaf-like surfaces through soft-lithographic imprinting. *Macromol. Rapid Commun.* **2006**, *27*, 1859–1864. [CrossRef]

30. Kim, M.R.; Lee, S.; Park, J.K.; Cho, K.Y. Golf ball-shaped PLGA microparticles with internal pores fabricated by simple O/W emulsion. *Chem. Commun.* **2010**, *46*, 7433–7435. [CrossRef] [PubMed]
31. Zhang, Q.C.; Liu, J.; Wang, X.J.; Li, M.X.; Yang, J. Controlling internal nanostructures of porous microspheres prepared via electrospraying. *Colloid Polym. Sci.* **2010**, *288*, 1385–1391. [CrossRef]
32. Vehring, R. Pharmaceutical particle engineering via spray drying. *Pharm. Res.* **2008**, *25*, 999–1022. [CrossRef] [PubMed]